

Chapter 1

Open heavy-flavour production in pp collisions



OPEN HEAVY-FLAVOUR hadrons, made of a heavy quark (charm or beauty) along with lighter quarks (e.g. D- and B-mesons), are exclusively formed in high-momentum transfer processes due to their the large mass of approximately $1.27 \text{ GeV}/c^2$ and $4.18 \text{ GeV}/c^2$ for charm and beauty quarks, respectively. As such, they are created in the early stages of the collision, and their production cross-section in the partonic interaction can be evaluated perturbatively using QCD. Studying the production of open heavy-flavour hadrons in proton-proton collisions not only provides a crucial test of the perturbative QCD framework, but also allows to set constraints on models. Furthermore, such measurements in proton-proton collisions, where the production of a deconfined medium is not expected due to the low energy densities reached, are necessary ingredients for the study of heavy-ion collisions, where the properties of the QGP can be investigated.

1.1 Factorisation theorems

The production of open heavy-flavour hadrons in proton-proton collisions can be described using the factorisation theorems [1], which allow for the separation of short-distance, perturbative behaviour from the long-distance, non-perturbative phenomena. The total production cross-section can be expressed as

$$\sigma_{pp} = \sum_{a,b=g,q,\bar{q}} \int dx_1 dx_2 f_{a/A}(x_1, \mu_F^2) f_{b/B}(x_2, \mu_F^2) \hat{\sigma}_{ab \rightarrow c}(x_1, x_2, \mu_F^2, \mu_R^2) D_{c \rightarrow H}(z, \mu_F^2) \quad ,$$

i.e. the convolution of; i. the Parton Distribution Functions (PDFs) $f_{a/A}(x_1, \mu_F^2)$ and $f_{b/B}(x_2, \mu_F^2)$, describing the probability of finding a parton a in the proton A carrying a fraction x_1 of the proton's momentum, and a parton b in the proton B carrying a fraction x_2 of its momentum, respectively; ii. the hard partonic scattering cross-section $\hat{\sigma}_{ab \rightarrow c}(x_1, x_2, \mu_F^2, \mu_R^2)$, defining the probability of producing the final state c from the collision of partons a and b; and iii. the Fragmentation Functions (FFs) $D_{c \rightarrow H}(z, \mu_F^2)$, which describe the probability of a parton of type c fragmenting into a

heavy-flavour hadron H with a momentum fraction z . While the PDFs and FFs are non-perturbative quantities, determined from experimental data and then regarded as universal across different processes, the hard partonic scattering cross-section can be perturbatively calculated using QCD, albeit requiring specific evaluations for each process. Factorisation theorems have been widely used to describe the production of open heavy-flavour hadrons in proton-proton collisions, and have proven to be successful in modeling experimental data. Figure 1.1 shows the production cross-section of prompt and non-prompt D^0 -mesons in proton-proton collisions at $\sqrt{s} = 13$ TeV measured at midrapidity ($|y| < 0.5$) as a function of the transverse momentum p_T by the ALICE experiment [2], and compared to FONLL calculations [3]. The term *prompt* refers to charm-hadrons directly produced in the hadronisation of a charm quark or through the strong decay of a directly produced excited charm-hadron state, while *feed-down* charm-hadrons are produced in the decay of a hadron containing a beauty quark. The FONLL predictions are in good agreement with the non-prompt D^0 -meson production cross-section, whereas the prompt contribution lies at the upper edge of the theoretical uncertainty band, albeit being described within the uncertainties. Similar trends are observed in the production of other open heavy-flavour hadrons across different experimental facilities, such as the Tevatron, RHIC and LHC.

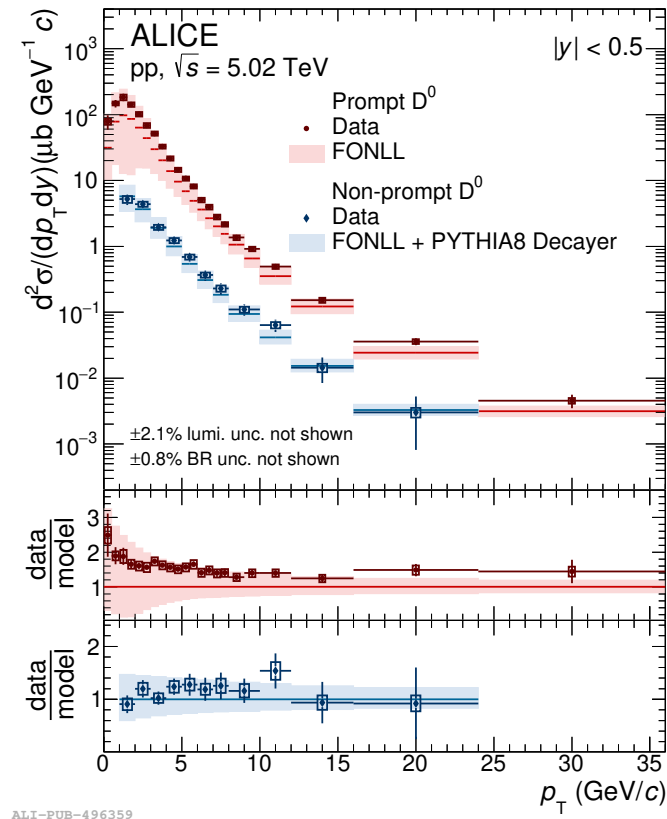


Figure 1.1: p_T -differential production cross-section of prompt and non-prompt D^0 -mesons [2] compared to predictions obtained with FONLL calculations [3] combined with PYTHIA 8 [4] for the $H_b \rightarrow D^0 + X$ decay kinematics.

1.1.1 Parton Distribution Functions

Deep inelastic scattering

The PDFs are non-perturbative quantities that describe the probability of finding a parton with a fraction x of the proton momentum in the initial state of the process. The experiment that provided the first evidence of the partonic structure of the proton was the deep inelastic scattering experiment carried out at the Stanford Linear Accelerator Center (SLAC) in the 1960s [5], where an electron was scattered off a proton, and the transferred momentum q was measured. The cross-section for deep inelastic scattering can be defined in terms of the Lorentz invariant variables $Q^2 = -q^2$ and $x = \frac{Q^2}{2P \cdot q}$, and are given by:

$$\frac{d^2\sigma}{dx dQ^2} = \frac{4\pi\alpha^2}{xQ^4} [(1-y) F_2(x, Q^2) - xy^2 F_1(x, Q^2)] \quad ,$$

where $y = Q^2/(sx)$, $s = (P + p_e)^2$ is the centre-of-mass energy of the e-p system. The structure functions $F_1(x, Q^2)$ and $F_2(x, Q^2)$ are an extension of the form factors for elastic scattering. The first measurements of high energy inclusive inelastic scattering experiments were carried out with a 20 GeV linear accelerator at SLAC, and showed that the structure functions $F_1(x, Q^2)$ and $F_2(x, Q^2)$ were independent of Q^2 at fixed x in the studied $1 < Q^2 < 10 \text{ GeV}/c^2$ range. This was in contrast to what was found for the proton elastic form factors, where a decrease of two orders of magnitude was observed in the same Q^2 interval. The observed behaviour was predicted by Bjorken in 1968 for $Q^2 \rightarrow \infty$ [6], and is known as *Bjorken scaling*. A physical interpretation of the phenomena arrived just one year later, in 1969, with Feynman's parton model [7], which described the interaction in terms of an elastic scattering of the probe off a point-like constituent (parton) of the proton. This explains the scale-invariance property of the proton structure functions, since the scattering centres are structure-less. In this picture, the Bjorken variable x gains a new interpretation as the fraction of the proton momentum carried by the struck parton. The parton model also provided with a simple definition of the structure functions in terms of the parton distribution functions $f_a(x)$:

$$F_2(x, Q^2) = \sum_a e_a^2 x f_a(x) \quad ,$$

where the sum is over partons with electric charge e_a , and f_a are unknown, but universal functions for a given hadron, describing the probability of finding a parton of type a with a fraction x of the proton momentum.

To study the spin properties of the partons, the structure functions F_1 and F_2 were studied at different centre-of-mass energies. By investigating the relationship between the two structure functions, it was established that the partons have spin $1/2$, as the Callan-Gross relation [8], which is true for point-like Dirac particles, was found to be satisfied:

$$F_2(x, Q^2) = 2xF_1(x, Q^2) \quad .$$

In the next years, it became clear that there must be other constituents in the proton carrying momentum, but not electric charge nor weak charge, as the so-called momentum sum rule was not saturated by the measured PDFs in electron

and neutrino scatterings. The missing momentum was attributed to the gluons, which were discovered in the 1970s and are the field quantum of the strong force.

Bjorken scaling violation

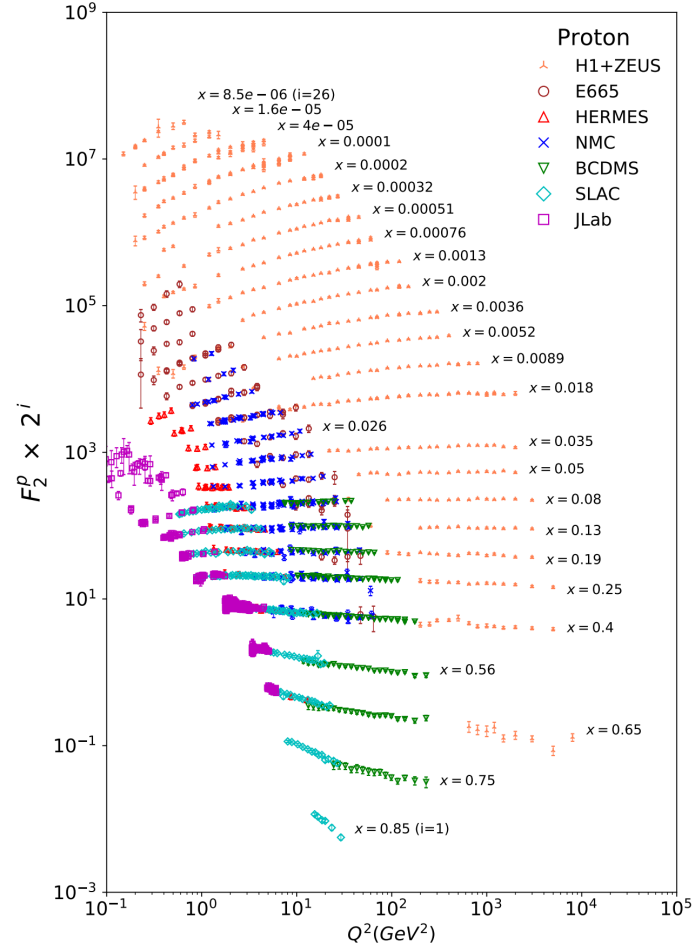


Figure 1.2: The proton structure function F_2^p measured in electromagnetic scattering of electrons and positrons on protons, and for electrons/positrons and muons on a fixed target [9].

By the end of the 1970s, measurements of the structure functions at larger Q^2 values taken at CERN and Desy showed that the Bjorken scaling was violated, i.e. the structure functions were not Q^2 independent. Figure 1.2 shows the measurements of proton structure functions $F_2(x, Q^2)$ as a function of Q^2 for different values of x by different experiments [9]. It is clear from the plot that structure functions present an increasing trend as a function of Q^2 at low x , and a decreasing trend as a function of Q^2 at high x . The parton model is not able to explain this behaviour as it relies on the assumption that the transferred energy is large enough to neglect the mass of the proton and its constituents, and the interactions between the partons. In particular, the partons' transverse momentum with respect to the proton momentum is neglected. The key point in understanding the Bjorken scaling violation comes from QCD and is that the parton's transverse

momentum is not in fact restricted to be small. A quark can emit a gluon and acquire large transverse momentum k_T with a probability proportional to $\alpha_s dk_T/k_T^2$ at large k_T . The integral extends up to the kinematic limit $k_T \sim Q^2$, and gives rise to contributions proportional to $\alpha_s \log Q^2$, which break scaling. The evolution of the PDFs with Q^2 from a parametrisation at a given Q_0^2 can be perturbatively described using the Dokshitzer-Gribov-Lipatov-Altarelli-Parisi (DGLAP) evolution equations [10, 11, 12], which requires introducing a new arbitrary scale, at which the factorisation of the perturbative processes happens: the factorisation scale μ_F .

There exists a wide range of PDFs parametrisations, such as the NNPDF [13], CTEQ [14] and MMHT [15], which are determined from global fits to a wide range of experimental data, such as deep inelastic scattering, Drell-Yan, and jet production.

1.1.2 Partonic cross-section

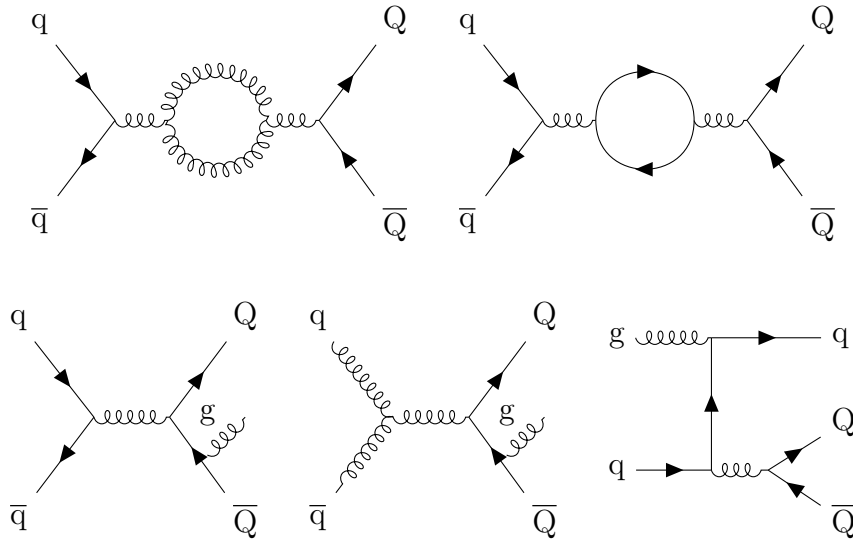


Figure 1.3: Feynman diagrams contributing to the first order corrections of the heavy-flavour production cross-section calculations.

Because of their large masses, heavy quarks can only be produced in hard-scattering processes, with momentum transfer of the order of $Q^2 \geq 4m_{b,c}^2$. The strong coupling constant is significantly smaller than unity in this regime, and the production cross-section of heavy quarks from partonic scattering can be calculated perturbatively using QCD. Although for some processes, such as Higgs production, predictions at next-to-next-to-next-to-leading order (N³LO) are available [16, 17], for heavy quark production, the state-of-the-art calculations are available at next-to-leading order (NLO) with all-order resummation to next-to-leading log (NLL) accuracy in the limit where the p_T of a heavy quark is much larger than its mass [18]. The contributions arising at the NLO include 1-loop virtual corrections to the Born process and real emission of a gluon, and are reported in Fig 1.3.

1.1.3 Fragmentation Functions

The Fragmentation Functions $D_{c \rightarrow H}(z, \mu_F^2)$ describe the probability of a parton of type c fragmenting into a hadron H with a momentum fraction z . They are non-perturbative quantities that encapsulate the hadronisation process, where partons transform into observable hadrons. FFs are typically determined from experimental data, usually by analyzing the final-state hadrons produced in electron-positron collisions, where the initial momenta are well-known. By studying the distribution of identified hadrons as a function of their momentum fraction z , researchers can extract information about the fragmentation process. As for the PDFs, also the FFs evolve with the energy scale of the interaction and this evolution is described by the DGLAP equations.

1.2 Modification of the hadronisation mechanism

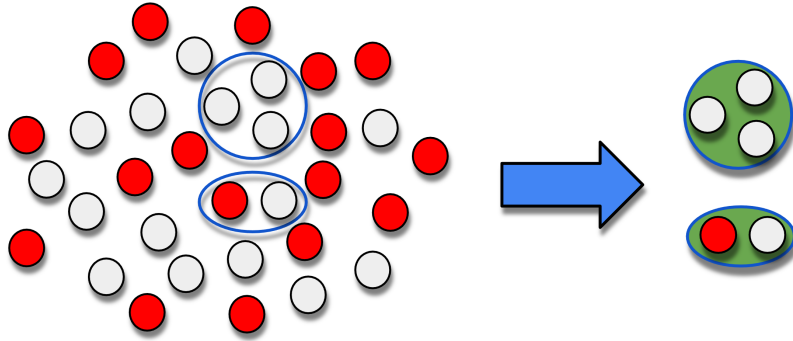


Figure 1.4: Representation of hadron production via recombination.

As briefly described in Sec. ??, the hadronisation process can be modified in the presence of a strongly-interacting deconfined medium. A new mechanism for the production of hadrons, the recombination, can take place in the QGP. This process modifies the production of hadrons in heavy-ion collisions, so that the description of fragmentation functions provided by e^+e^- collisions is not valid anymore. Only models implementing the coalescence mechanism manage to describe the production of hadrons in these collisions. Even more, models implementing recombination that successfully describe the production of hadrons in heavy-ion collisions, fail in doing so when this process is de-activated, as shown in Fig. 1.5. Measurements of charm-baryons production in proton-proton and proton-lead collisions [19, 20] have provided interesting results on the production of hadrons in these systems, as models with hadronisation tuned on e^+e^- collisions fail to describe the data. This observation may suggest that coalescence could also play a role in small collision systems, and that the hadronisation process is not universal across different systems at all.

Different models have been developed in order to describe this baryon enhancement in proton-proton, such as SHM+RQM [22, 23], where a strong feed-down from an augmented set of excited charm- or beauty-baryon states is considered; the Quark (re-)Combination Mechanism [24] model, where coalescence between a

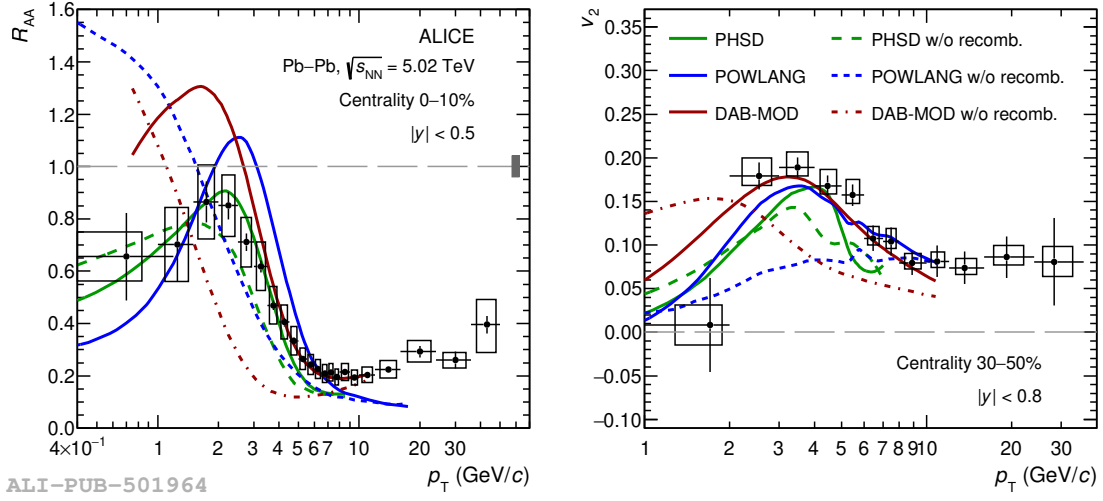


Figure 1.5: Prompt D-meson R_{AA} in the 0–10% centrality class (left panel) and v_2 in the 30–50% centrality class (right panel) compared with predictions obtained with and without including hadronisation via recombination. Taken from [21].

charm quark and an equal-velocity light quarks from fragmentation takes place, and thermal weights are applied to account for relative production of scalar and vector mesons; the Catania coalescence model [25], which describes a thermalised system of u , d , s quarks and gluons, and the charm quark can hadronize either via fragmentation or coalescence with light quarks from the bulk; and, lastly, the POWLANG model [26], where a small, deconfined and expanding fireball is expected to form in proton-proton collisions, and charm quark are subject to rescattering and hadronization and can recombine with light quarks, as in heavy-ion collisions. Each of these models provides a different hadronization mechanism in proton-proton collisions compared to e^+e^- ones, and independent hadronization is no longer assumed.

The influence of the surrounding environment in the hadronisation of the charm quark could also potentially explain the observed strangeness enhancement in proton-proton collisions. If many strange quarks are produced in the same region as the charm quark, the probability of recombination between the two is higher, and the production of charm-strange hadrons is enhanced. This phenomena can be studied by measuring the production yield ratio of charm-strange hadrons to non-strange charm hadrons, such as the D_s^+ -meson to D^+ -meson ratio, which will be the main focus of this Thesis.

Bibliography

- [1] J. C. Collins, D. E. Soper, and G. F. Sterman, “Factorization of Hard Processes in QCD”, *Adv. Ser. Direct. High Energy Phys.* **5** (1989) 1–91, [arXiv:hep-ph/0409313](#).
- [2] **ALICE** Collaboration, S. Acharya *et al.*, “Measurement of beauty and charm production in pp collisions at $\sqrt{s} = 5.02$ TeV via non-prompt and prompt D mesons”, *JHEP* **05** (2021) 220, [arXiv:2102.13601 \[nucl-ex\]](#).
- [3] M. Cacciari, S. Frixione, and P. Nason, “The p(T) spectrum in heavy flavor photoproduction”, *JHEP* **03** (2001) 006, [arXiv:hep-ph/0102134](#).
- [4] T. Sjöstrand, S. Ask, J. R. Christiansen, R. Corke, N. Desai, P. Ilten, S. Mrenna, S. Prestel, C. O. Rasmussen, and P. Z. Skands, “An introduction to PYTHIA 8.2”, *Comput. Phys. Commun.* **191** (2015) 159–177, [arXiv:1410.3012 \[hep-ph\]](#).
- [5] J. I. Friedman and H. W. Kendall, “Deep inelastic electron scattering”, *Ann. Rev. Nucl. Part. Sci.* **22** (1972) 203–254.
- [6] J. D. Bjorken, “Asymptotic Sum Rules at Infinite Momentum”, *Phys. Rev.* **179** (1969) 1547–1553.
- [7] R. P. Feynman, “Very high-energy collisions of hadrons”, *Phys. Rev. Lett.* **23** (1969) 1415–1417.
- [8] C. G. Callan, Jr. and D. J. Gross, “High-energy electroproduction and the constitution of the electric current”, *Phys. Rev. Lett.* **22** (1969) 156–159.
- [9] **Particle Data Group** Collaboration, R. L. Workman and Others, “Review of Particle Physics”, *PTEP* **2022** (2022) 083C01.
- [10] V. N. Gribov and L. N. Lipatov, “Deep inelastic e p scattering in perturbation theory”, *Sov. J. Nucl. Phys.* **15** (1972) 438–450.
- [11] Y. L. Dokshitzer, “Calculation of the Structure Functions for Deep Inelastic Scattering and e+ e- Annihilation by Perturbation Theory in Quantum Chromodynamics.”, *Sov. Phys. JETP* **46** (1977) 641–653.
- [12] G. Altarelli and G. Parisi, “Asymptotic Freedom in Parton Language”, *Nucl. Phys. B* **126** (1977) 298–318.

- [13] **NNPDF** Collaboration, R. D. Ball *et al.*, “The path to proton structure at 1% accuracy”, *Eur. Phys. J. C* **82** (2022) 428, [arXiv:2109.02653 \[hep-ph\]](#).
- [14] S. Dulat, T.-J. Hou, J. Gao, M. Guzzi, J. Huston, P. Nadolsky, J. Pumplin, C. Schmidt, D. Stump, and C. P. Yuan, “New parton distribution functions from a global analysis of quantum chromodynamics”, *Phys. Rev. D* **93** (2016) 033006, [arXiv:1506.07443 \[hep-ph\]](#).
- [15] L. A. Harland-Lang, A. D. Martin, P. Motylinski, and R. S. Thorne, “Parton distributions in the LHC era: MMHT 2014 PDFs”, *Eur. Phys. J. C* **75** (2015) 204, [arXiv:1412.3989 \[hep-ph\]](#).
- [16] C. Anastasiou, C. Duhr, F. Dulat, F. Herzog, and B. Mistlberger, “Higgs Boson Gluon-Fusion Production in QCD at Three Loops”, *Phys. Rev. Lett.* **114** (2015) 212001, [arXiv:1503.06056 \[hep-ph\]](#).
- [17] C. Anastasiou, C. Duhr, F. Dulat, E. Furlan, T. Gehrmann, F. Herzog, A. Lazopoulos, and B. Mistlberger, “High precision determination of the gluon fusion Higgs boson cross-section at the LHC”, *JHEP* **05** (2016) 058, [arXiv:1602.00695 \[hep-ph\]](#).
- [18] M. Cacciari, M. Greco, and P. Nason, “The p_T spectrum in heavy-flavour hadroproduction.”, *JHEP* **05** (1998) 007, [arXiv:hep-ph/9803400](#).
- [19] **ALICE** Collaboration, S. Acharya *et al.*, “First measurement of Λ_c + production down to $p_T=0$ in pp and p-Pb collisions at $\sqrt{s_{NN}}=5.02$ TeV”, *Phys. Rev. C* **107** (2023) 064901, [arXiv:2211.14032 \[nucl-ex\]](#).
- [20] **ALICE** Collaboration, S. Acharya *et al.*, “Measurement of the production cross section of prompt Ξ_c^0 baryons in p-Pb collisions at $\sqrt{s_{NN}} = 5.02$ TeV”, To be published.
- [21] **ALICE** Collaboration, S. Acharya *et al.*, “Prompt D^0 , D^+ , and D^{*+} production in Pb-Pb collisions at $\sqrt{s_{NN}} = 5.02$ TeV”, *JHEP* **01** (2022) 174, [arXiv:2110.09420 \[nucl-ex\]](#).
- [22] M. He and R. Rapp, “Charm-Baryon Production in Proton-Proton Collisions”, *Phys. Lett. B* **795** (2019) 117–121, [arXiv:1902.08889 \[nucl-th\]](#).
- [23] M. He and R. Rapp, “Bottom Hadrochemistry in High-Energy Hadronic Collisions”, *Phys. Rev. Lett.* **131** (2023) 012301, [arXiv:2209.13419 \[hep-ph\]](#).
- [24] J. Song, H.-h. Li, and F.-l. Shao, “New feature of low p_T charm quark hadronization in pp collisions at $\sqrt{s} = 7$ TeV”, *Eur. Phys. J. C* **78** (2018) 344, [arXiv:1801.09402 \[hep-ph\]](#).
- [25] V. Minissale, S. Plumari, and V. Greco, “Charm hadrons in pp collisions at LHC energy within a coalescence plus fragmentation approach”, *Phys. Lett. B* **821** (2021) 136622, [arXiv:2012.12001 \[hep-ph\]](#).

- [26] A. Beraudo, A. De Pace, D. Pablos, F. Prino, M. Monteno, and M. Nardi, “Heavy-flavor transport and hadronization in pp collisions”, *Phys. Rev. D* **109** (2024) L011501, [arXiv:2306.02152](#) [hep-ph].